An International Journal
computers & mathematics with applications

PERGAMON Computers and Mathematics with Applications 45 (2003) 1883–1894
www.elsevier.com/locate/camwa

A Fast Quasi-Multiple Medium Method for 3-D BEM Calculation of Parasitic Capacitance

WENJIAN YU* AND ZEYI WANG
Department of Computer Science and Technology, Tsinghua University
Beijing 100084, P.R. China
ywj77@computer.org

(Received December 2001; accepted January 2002)

Abstract—A quasi-multiple medium (QMM) method is proposed to accelerate the boundary element method (BEM) for the 3-D parasitic capacitance calculation. In the QMM method, a homogeneous dielectric is decomposed into a number of fictitious medium blocks, each with the same permittivity of original medium. By the localization character of BEM, the QMM method makes great sparsity to the coefficient matrix of the overall discretized BEM equations. Then, using storing technique of sparse matrix and iterative equation solvers, the sparsity is explored to greatly reduce CPU time and memory usage of BEM computation. The computational complexity of the QMM accelerated BEM for a single-medium model problem is analyzed, and it is concluded as $O(N)$, if the number of iterations is bounded. Numerical results verify the theoretical analysis and show the accelerating efficiency of the QMM method for calculation of 3-D parasitic capacitance.

Keywords—Quasi-multiple medium, Boundary element method, Laplace equation, 3-D parasitic capacitance calculation.

1. INTRODUCTION

Efficient and precise solution of the Laplace equation is of great significance in scientific and engineering computation because the behavior of many physical systems is governed by it. The direct boundary element method (BEM), based on the direct boundary integral formulation [1], has been widely employed for solving the Laplace equation because of its ability to reduce the dimensionality of problems. The iterative solution of the discrete integral equations with N boundary variables generally takes operation of $O(N^2)$, when efficient Krylov subspace iterative solvers with preconditioning are used. For large values of N, this is also extremely expensive.

Since the mid-1980s, several rapid solution approaches [2–6] to integral equations from the classical potential theory and scattering theory have been proposed. At the same time, many hierarchical algorithms [7–9] were developed for rapid evaluation of Coulombic interaction in

This work is partly supported by the China National Science Foundation under Grant 69876024, and the China National Foundation for Key Basic Research under Grant G1998030404. The authors would like to thank them for their financial support.
*Author to whom all correspondence should be addressed.

0898-1221/03/$ - see front matter Typeset by $\mathcal{A}\mathcal{M}\mathcal{S}$-TEX
PII: S0898-1221(03)00178-0

large-scale particle assembly. Because of the similarity between the N-body simulation and boundary element solution, the hierarchical techniques developed for particle simulation are also applied to fast computation of dense matrix-vector product arising in BEM [10]. Recently, the famous multipole algorithm proposed by Rokhlin [2] continued to be improved [11–13], and some parallel versions [14,15] were presented.

In addition, we should emphasize the multizone boundary element technique whose early idea was briefly introduced by Kane and Kumar [16] and has been used for significantly extending the range of model shapes and optimizing shape in the design sensitivity analysis [17–19]. At the same time, the sparsity in the coefficient matrix of the discrete linear system produced by the multizone technique was attended and exploited for getting higher computational efficiency in [17,19]. But, it seems that the multizone boundary element analysis has not been treated as a fast solution to the direct boundary element method. In fact, the fast quasi-multiple medium (QMM) method proposed in this paper is similar to the multizone boundary element method, though their backgrounds are not the same. But in the QMM method, we utilize the boundary element analysis for multiple mediums and the iterative equation solver for large-scale computation, and are concerned with how a single medium should be decomposed so that computational speed-up can be obtained. In the application of parasitic capacitance extraction, the QMM method has shown its efficiency in reducing computing time and memory usage.

Today, in the deep submicron very large-scale integration (VLSI) circuits, the parasitic capacitance of interconnect conductors is becoming dominant in governing circuit performances such as time delay, power consumption, etc. Many rapid solutions mentioned above were successfully used to accelerate the boundary element evaluation of the parasitic capacitance [10,15,20]. But, it should be pointed out that all these algorithms were almost implemented in the indirect BEM and will encounter a lot of difficulties while extending them to the problem with multiple dielectrics and finite domain. Compared with the indirect BEM, the direct BEM is more convenient to treat the problems with the mixed Neumann and Dirichlet boundary conditions, because there are two variables of electrical potential and its normal derivative in the direct boundary integral equation (BIE) [1,19].

In this paper, a quasi-multiple medium (QMM) method is proposed to accelerate the direct BEM computation. It utilizes the localization character of direct BEM to transfer the coefficient matrix into a very sparse one. With the technique of storing sparse block matrix and the Krylov iterative solvers, the QMM method reduces the computing time and memory usage greatly. With a simplified model problem, the computational complexity of the QMM accelerated BEM is analyzed, and is concluded as a nearly linear relationship with the number of boundary elements. Two numerical experiments are presented. The first one is designed to verify the analysis of computational complexity, and the second one demonstrates the efficiency of the QMM method for the calculation of actual 3-D VLSI parasitic capacitance.

The rest of this paper is organized as follows. Section 2 outlines the direct BEM for calculation of parasitic capacitance. The QMM method and the analysis of its computational complexity are presented in Section 3. In Section 4, some numerical results are shown to demonstrate the performances of the QMM method. Finally, we give conclusions in Section 5.

2. DIRECT BEM CALCULATION OF PARASITIC CAPACITANCE

The formulations of direct BEM are reviewed for a potential problem, the calculation of VLSI parasitic capacitance. The parasitic capacitance can be obtained through the computation of normal electrical field intensity on surfaces of conductors [20]. In the three-dimensional domain Ω of a parasitic capacitor with single dielectric, electrical potential u fulfills the Laplace equation with mixed boundary conditions

$$\begin{aligned} \nabla^2 u = \frac{\partial^2 u}{\partial x^2} + \frac{\partial^2 u}{\partial y^2} + \frac{\partial^2 u}{\partial z^2} = 0, \qquad & \text{in } \Omega, \\ u = u_0, & \text{on } \Gamma_u, \\ q = \frac{\partial u}{\partial \mathbf{n}} = q_0 = 0, & \text{on } \Gamma_q, \end{aligned} \tag{1}$$

where ε is the permittivity of the dielectric. Γ_u is the surface of conductors, where u is known and determined by bias voltages; Γ_q is the Neumann boundary (outer boundary of the dielectric), where normal electrical field intensity q is supposed to be zero. $\mathbf{n}$ stands for the unit vector outward normal to the boundary. $\partial\Omega = \Gamma_u \cup \Gamma_q$ is the boundary surrounding the domain Ω, which is filled by the dielectric.

With the fundamental solution u^* of the Laplace equation as weight function, the Laplace equation in (1) is transformed into following direct BIE by the Green's formula [1]:

$$c_s u_s + \int_{\partial\Omega} q^* \, u \, d\Gamma = \int_{\partial\Omega} u^* \, q \, d\Gamma, \tag{2}$$

where u_s is the electrical potential at source point s, c_s is a constant dependent on boundary geometry near the point s, and q^* is the derivative of u^* along the outward normal direction of boundary $\partial\Omega$.

Employing constant quadrilateral elements, we obtain the discretized BIE. By evaluating it at every collocation point k, one for an element, the whole discretized BIEs are obtained as

$$c_k u_k + \sum_{j=1}^{N} \left(\int_{\Gamma_j} q^*_{(k)} \, d\Gamma \right) u_j = \sum_{j=1}^{N} \left(\int_{\Gamma_j} u^*_{(k)} \, d\Gamma \right) q_j, \qquad k = 1, \ldots, N, \tag{3}$$

where N is the number of boundary elements, and Γ_j is the j^{th} element. With a certain setting of bias voltages, the discretized BIEs can be written as

$$\mathbf{A}\mathbf{x} = \mathbf{f}, \tag{4}$$

where vector $\mathbf{x}$ includes all discretized variables, the unknowns of electrical potential on the outer dielectric surfaces, and normal electrical field intensity on the conductor surfaces.

For a large-scale 3-D problem, the coefficient matrix $\mathbf{A}$ is a large nonsymmetric matrix. The Krylov iterative solvers with preconditioning are usually efficient to solve this kind of equation [21]. A GMRES algorithm [22] with diagonal preconditioning is used in this paper. Then, the parasitic capacitance can be evaluated by the integral of normal electrical field intensity on the conductor surfaces [20].

For a problem with multimedium domains $\Omega = \cup\Omega_i$ $(i = 1, \ldots, M)$, where M is the number of mediums, the electrical potential u and its normal derivative q need to fulfill the compatibility equations along the interfaces Γ_I of two adjacent mediums a and b,

$$\varepsilon_a \frac{\partial u_a}{\partial \mathbf{n}_a} = -\varepsilon_b \frac{\partial u_b}{\partial \mathbf{n}_b}, \quad u_a = u_b, \qquad \text{on } \Gamma_I, \tag{5}$$

where ε_a and ε_b stand for the permittivities of medium a and b. The u and q on the interfaces are both unknown. Thus, the boundary of each medium in the multimedium system is the combination of three kinds of boundary, including Γ_u, Γ_q, and Γ_I.

Equation (3) for each medium can be put together utilizing the compatibility equations (5). Then, a coupled system of linear equations with the same form of (4) is obtained, where $\mathbf{x}$ involves all kinds of discretized variables, including the unknowns of u and q on the interfaces.

3. QUASI-MULTIPLE MEDIUM METHOD

3.1. Localization Character of Direct BEM

From formulas (3) and (5) we can see that in each discretized BIE all the discretized variables are on boundary elements of one dielectric region. So, for a problem with multiple mediums, there are direct interactions among the boundary elements in the same medium, which result in nonzero coefficients in the overall equation (4). We call this the localization character of direct BEM.

In the linear system (4), coefficient matrix **A** reflects the distribution of interactions among all boundary elements. If there is the direct interaction between two elements, nonzero entries are formed by the integrals in (3), which are taken on one of the elements with the source point on the other. Otherwise, when the source point and the discrete variables are on the elements without direct interaction, i.e., not involved in a same medium, zero entries are formed in the matrix. For a problem with multiple mediums, the localization of direct BEM makes matrix **A** sparse, from which we could benefit while solving the system of algebraic equations (4). In Figure 1, we show a typical capacitor with two mediums and the corresponding matrix **A** generated by the direct BEM, where the nonzero entries and the owners of discrete variables are indicated.

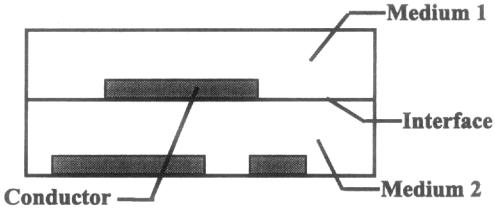

(a) A two-dimensional problem with two mediums.

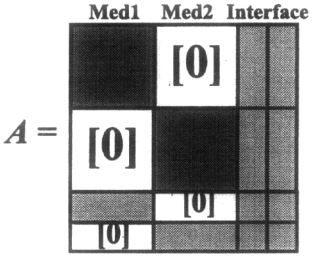

(b) The corresponding coefficient matrix A, where the gray blocks stand for nonzero entries.

Figure 1.

3.2. Quasi-Multiple Medium Method

The QMM method takes full advantage of the localization character of direct BEM. A single medium with permittivity ε is regarded as a composition of Q fictitious medium blocks, whose permittivities are all the same as ε, as shown in Figure 2. Thus, the problem with single medium is transferred into a problem with some fictitious mediums. Because of the localization character, the dense coefficient matrix for a single-medium problem is converted into a sparse one for the problem with multiple mediums.

With suitable decomposition of the single medium, the resulting coefficient matrix **A** will become one with much sparsity so that computational speed-up is available. With the storage technique of sparse blocked matrix and iterative equation solvers such as the GMRES algorithm, the computing time and memory usage for the original single medium problem will be greatly reduced. We call this the quasi-multiple medium (QMM) method. The QMM method is not only useful for single-medium problems, but also for multimedium problems, because the idea of decomposing each medium is also applicable to problems with multiple mediums.

Therefore, the QMM method includes the following three main points. First, a single medium is regarded as a composition of some fictitious mediums. Second, a suitable strategy of decomposition is considered to make the resulting BEM coefficient matrix with much sparsity. Last, the technique of storing sparse matrix and iterative equation solver are used to benefit from the matrix sparsity.

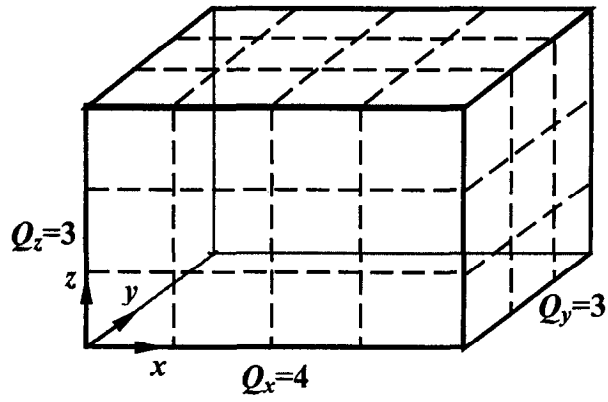

Figure 2. A single dielectric with Cartesian coordinate system is cut into $Q = Qx \cdot Qy \cdot Qz$ fictitious mediums.

It should be pointed out that the QMM method adds some unknowns to the overall problem, which are introduced on the additional fictitious interfaces of quasi-multiple mediums. For the calculation of parasitic capacitance, these unknowns account for a little percentage of total unknowns since most boundary elements are located on the conductor surfaces, generally. So, the advantage taken from the sparsity of the coefficient matrix might greatly outweigh the disadvantage of adding some unknowns.

3.3. Analysis of Computational Complexity

In this section, we first discuss the importance of the number of the nonzero matrix entries for large-scale BEM computation. Then, the computational complexity of QMM method is analyzed for the optimal situation.

The total CPU time used in large-scale BEM computation can be expressed as follows:

$$t = t_{\text{gen}} + t_{\text{sol}} + t_{\text{aux}}, \tag{6}$$

where t_{gen} is the time spent in generation of the coefficients in equation (4), t_{sol} is the time spent in solution of equation (4), and t_{aux} stands for the time spent in other supplementary procedures, including input of structure data and partition of boundary elements, etc. Generally speaking, the sum of t_{gen} and t_{sol} accounts for most part of the total CPU time t. Using the iterative equation solvers such as GMRES [22], we can then get the following nearly linear relationships:

$$t_{\text{gen}} \propto Z, \qquad t_{\text{sol}} \propto Zl, \tag{7}$$

where Z stands for the number of nonzero entries of matrix $\mathbf{A}$, and l stands for the number of iterations.

For a large 3-D problem, the coefficient matrix $\mathbf{A}$ is a nonsymmetric matrix with a large order. The GMRES algorithm is suitable for this kind of equation, and a good preconditioning matrix should also be selected to quicken its convergence [21]. When organizing the discretized BIEs, we make the order of the source points consistent with that of the discretized unknowns, so that the diagonal entries of the matrix are obtained by the singular integrals, in which the source point is within the element where the integral is taken. Because the singular integral results in a nonzero entry with very large absolute value, the diagonal preconditioner is adopted to bring quick convergence. So, the number of iterations is much less than the parameter Z in (7).

If we ignore the influence of t_{aux} and assume the l does not change much while using the QMM method, the speed-up ratio of the BEM computation with QMM acceleration to that without QMM acceleration is

$$R_{\text{speed-up}} = \frac{t}{t'} \approx \frac{Z}{Z'}, \tag{8}$$

where Z and Z' stand for the number of nonzero entries of matrix $\mathbf{A}$ in these two situations, respectively. This expression reveals that the ratio of numbers of nonzero matrix entries approximately equals the speed-up ratio of the QMM method.

Below, we analyze the number of nonzero entries in QMM computation, and compare it with that in the original single medium (SM) computation. Because of much difficulty in analyzing the general complex situation, a simplified model problem is discussed.

We suppose that there are N_s boundary elements uniformly distributed in the original single medium domain Ω_s; on each element, there is only discretized unknown. For simplicity, the configuration of the N_s boundary elements in the original single medium situation is not changed in the implementation of QMM. Hence, there are N_s/Q first kind boundary elements (on each one of which there is only one unknown) within each fictitious medium block, that is denoted by

$$\left|E_k^1\right| = \frac{N_s}{Q}, \qquad k = 1, \ldots, Q. \tag{9}$$

The number of interface surfaces is different for the Q fictitious medium blocks. For example, there are only three interfaces in the block located at eight vertices of the original rectangular parallelepiped, while six in the central blocks (see Figure 2). For simplicity, we conservatively assume that all the fictitious medium blocks have six interfaces, and the number of boundary elements on six interfaces is b. On each of these elements, there are two discretized unknowns. We call the boundary element with two unknowns the second kind of boundary element. So, the following expression is obtained:

$$\left|E_k^2\right| = b, \qquad k = 1, \ldots, Q. \tag{10}$$

According to formula (3) and the constant collocation method, the following number of nonzero entries is produced in the matrix $\mathbf{A}$ for each fictitious medium:

$$e_k = e = \left(\frac{N_s}{Q} + b\right)\left(\frac{N_s}{Q} + 2b\right), \qquad k = 1, \ldots, Q. \tag{11}$$

Then, the total number of nonzero entries in the QMM computation is

$$Z_Q = Q \cdot e = \frac{N_s^2}{Q} + 3N_s b + 2Qb^2. \tag{12}$$

We use Z_s to denote the number of the nonzero entries of coefficient matrix $\mathbf{A}$ in the original single-medium computation and have $Z_s = N_s^2$. Therefore, the speed-up ratio R brought by the QMM method is

$$R = \frac{Z_S}{Z_Q} = \frac{1}{1/Q + 3(b/N_s) + 2(b/N_s)^2 Q}. \tag{13}$$

Letting $c = b/N_s$, formula (13) can be rewritten as

$$R = \frac{1}{1/Q + 3c + 2c^2 Q}. \tag{14}$$

An optimal value of Q can be derived by

$$\frac{d}{dQ}\left(\frac{1}{Q} + 3c + 2c^2 Q\right) = 0, \tag{15}$$

and is obtained as

$$\tilde{Q} = \frac{\sqrt{2}}{2}\frac{1}{c} = \frac{\sqrt{2}}{2}\frac{N_s}{b}. \tag{16}$$

When the optimal $\tilde{Q}$ is used in the QMM computation, a maximal R can be obtained as follows:

$$R_{\max} = \frac{1}{2\sqrt{2}c + 3c} = \frac{1}{(3 + 2\sqrt{2})} \frac{N_s}{b}. \tag{17}$$

Because N_s is much larger than b, $R_{\max}$ is much larger than one. So, substantial computational speed-up is available.

From formulae (12) and (16), the minimal value of Z_Q, the number of nonzero entries of the coefficient matrix $\mathbf{A}$ in QMM computation, is obtained as

$$Z_{Q,\min} = \left[\left(2\sqrt{2} + 3\right) b\right] N_s. \tag{18}$$

Fixing the value of parameter c, formula (17) presents the maximal computational speed-up ratio of the QMM method to the SM computation. Furthermore, if the number of iterations in GMRES is bounded, we can see the linear relationship between CPU time of QMM computation and the number of boundary elements in the problem from formula (18). In addition, the number of boundary elements on the fictitious interfaces influences the value of parameter c, so it is very important for balancing the computational accuracy and speed of the QMM method.

4. NUMERICAL RESULTS

In this section, two experiments are carried out to demonstrate the efficiency of the QMM method. In the first experiment, a single-medium structure is designed to verify the analysis of the computational complexity of the QMM method. Actual parasitic capacitors with three dielectrics and crossover conductors are calculated with QMM accelerated BEM in the second experiment. Numerical results show that the QMM method greatly accelerates the direct BEM computation for parasitic capacitance, and the memory usage is reduced at the same time. The problems are run on a Sun-Ultra Enterprise 450 Server, and the stopping criteria of the GMRES is set to be 1.0×10^{-4}. In all data tables the unit of time is seconds, and the unit of capacitance is 10^{-18} farad. The unit of memory is megabytes.

4.1. $k \times k \times k$ Metal Cuboids Embedded in a Dielectric

Capacitors with $k \times k \times k$ (k = 2–8) metal cuboids distributed uniformly in a dielectric are used for the numerical experiment. The size of each metal cuboid is $0.4 \times 0.4 \times 0.4$ (unit in μm), and the size of the dielectric is $k \times k \times k$ (unit in μm). The relative permittivity of the dielectric is 3.9. The spacing between any two adjacent metal blocks is 0.6 μm. The capacitor with $2 \times 2 \times 2$ metal cuboids is shown in Figure 3a.

In the capacitors, one of the $k \times k \times k$ metal blocks is specified as the master conductor (whose bias voltage is 1 V), while the others are the environment conductors (whose bias voltages are all 0 V). We need to calculate the capacitance between the master and all environment conductors.

These structures can be calculated by direct BEM for single medium, which is called the SM computation. In the SM computation, there are four boundary elements on each surface of environment conductors, and nine elements on each surface of the master conductor. On each outer boundary surface of the dielectric with the size of $k \times k\,\mu\text{m}^2$, $2k \times 2k$ boundary elements are partitioned. On each of these boundary surfaces, boundary elements are partitioned uniformly. Using the idea of QMM method, these single-medium structures are decomposed into some fictitious medium blocks like Figure 2. We assume there are four boundary elements on each fictitious interface, and then the parameter b in (10) is 24. With the formula (16), we can get the theoretical optimal value of the number of fictitious mediums in QMM computation. They are denoted by $\tilde{Q}_k$ (k = 2–8) and listed in Table 1. According to the symmetry of these 3-D structures, the numbers of fictitious medium blocks along directions of the X-, Y-, and Z-axis

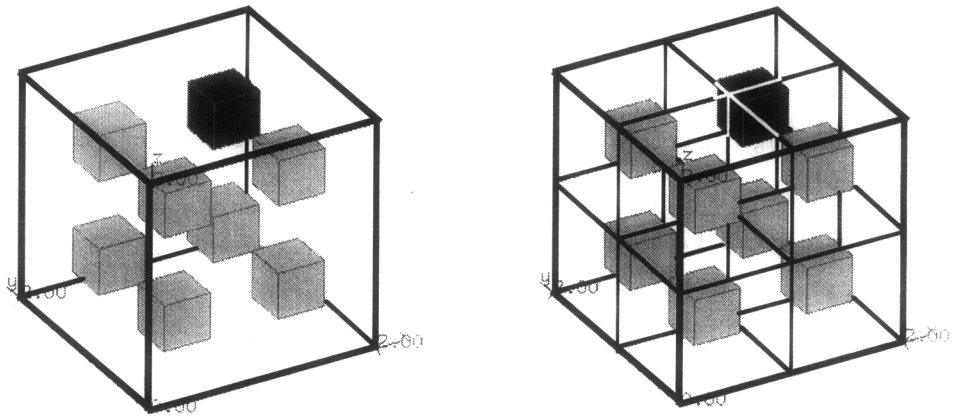

(a) A capacitor with $2 \times 2 \times 2$ metal cuboids, where the dark cuboid is the master conductor.

(b) The capacitor shown in (a) is divided into $2 \times 2 \times 2$ fictitious medium blocks.

Figure 3.

Table 1. Theoretical and actually adopted numbers of fictitious medium blocks along each axis for capacitor k ($k = 2$–8).

$k \times k \times k$	N-BE in SM[a]	Theoretical Value $\tilde{Q}_k$	Theoretical Value $\sqrt[3]{\tilde{Q}_k}$	Actual N-FMBEA[b]
$2 \times 2 \times 2$	318	9.37	2.1	2
$3 \times 3 \times 3$	894	26.34	3.0	3
$4 \times 4 \times 4$	1950	57.45	3.9	4
$5 \times 5 \times 5$	3630	106.95	4.7	5
$6 \times 6 \times 6$	6078	179.08	5.6	6
$7 \times 7 \times 7$	9438	278.07	6.5	7
$8 \times 8 \times 8$	13854	408.18	7.4	8

[a]N-BE in SM—number of boundary elements in SM computation.

[b]N-FMBEA—number of fictitious medium blocks along each axis.

are all the cube root of $\tilde{Q}_k$. They are also listed in Table 1, with the actually adopted numbers of fictitious medium blocks along each axis.

In our experiment, these optimal fictitious block numbers $\tilde{Q}_k$ are used to construct quasi-multiple medium structures. Except for the case with $8 \times 8 \times 8$ metal cuboids, we let the number of fictitious medium blocks along each direction be eight, in order to avoid processing complex boundary geometry.

Now, in this experiment the capacitor with $k \times k \times k$ metal cuboids is uniformly divided into $k \times k \times k$ fictitious blocks for QMM computation. Corresponding quasi-multiple medium structure of the capacitor with $2 \times 2 \times 2$ metal cuboids is shown in Figure 3b. In the QMM computation, the distribution of elements in the original SM computation is not changed. And, on each fictitious interface of mediums, four elements are added. The results of SM computation and QMM computation for these cases are listed in Table 2.

Table 2 shows the number of iterations, capacitance, and CPU time in the QMM computations compared with those in the SM computations. The QMM computation is at most about 50 times faster than SM computation. The discrepancies between the results obtained with SM computation and QMM computation are within 3%. The GMRES iterations increase for several steps in the QMM computations than in SM computations. This weakens the efficiency of the

Table 2. Comparison of the results between QMM computation and SM computation for capacitors with $k \times k \times k$ metal cuboids.

$k \times k \times k$	SM				QMM			Speed-Up Ratio	Dis.[d] (%)
	N-BE[a]	Iteration[b]	Cap.[c]	Time	N-BE[a]	Iteration[b]	Time		
$2 \times 2 \times 2$	318	7	94.6	1.2	366	13	0.4	3.0	2.5
$3 \times 3 \times 3$	894	9	117.1	8.9	1110	17	1.5	5.9	2.2
$4 \times 4 \times 4$	1950	10	148.3	41.1	2526	18	3.7	11.1	1.4
$5 \times 5 \times 5$	3630	12	148.3	152.5	4830	18	8.2	18.6	1.4
$6 \times 6 \times 6$	6078	13	148.3	405.6	8238	19	14.3	28.4	1.4
$7 \times 7 \times 7$	9438	14	148.3	1071.5	12966	19	24.4	43.9	1.4
$8 \times 8 \times 8$	13854	16	148.3	2214.2	19230	19	40.4	54.8	1.5

[a]N-BE—number of boundary elements.

[b]Iteration—the required number of iterations.

[c]Cap.—capacitance value, unit is 10^{-18}f.

[d]Dis.—the discrepancy of results by SM and QMM computations.

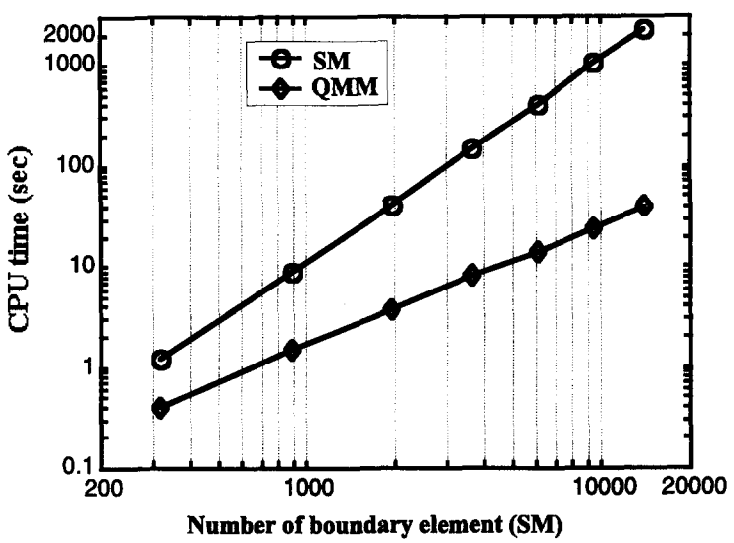

Figure 4. The log-log graph of the CPU time versus number of the boundary elements for a clear comparison of the computational complexity between the QMM and SM computations.

QMM method. From these results, it is clear to see that the bigger problem size is, the larger computational speed-up the QMM has.

We depict the relationship between the CPU time and size of simulated problem, which is represented by the number of boundary elements in SM computation, in a log-log graph (see Figure 4). From it, the power law for CPU time versus the number of boundary elements is found to be

$$\text{CPU time} \propto N^{2.00} \quad \text{(SM computation)},$$
$$\text{CPU time} \propto N^{1.21} \quad \text{(QMM computation)}.$$

This means the QMM algorithm has an approximately linear computational complexity, while the computational complexity of the SM computation is quadric.

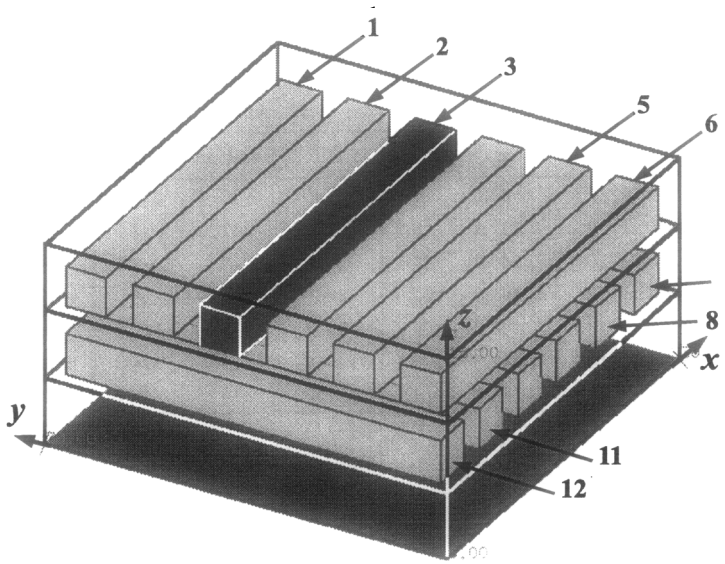

Figure 5. A structure with 6 × 6 crossovers.

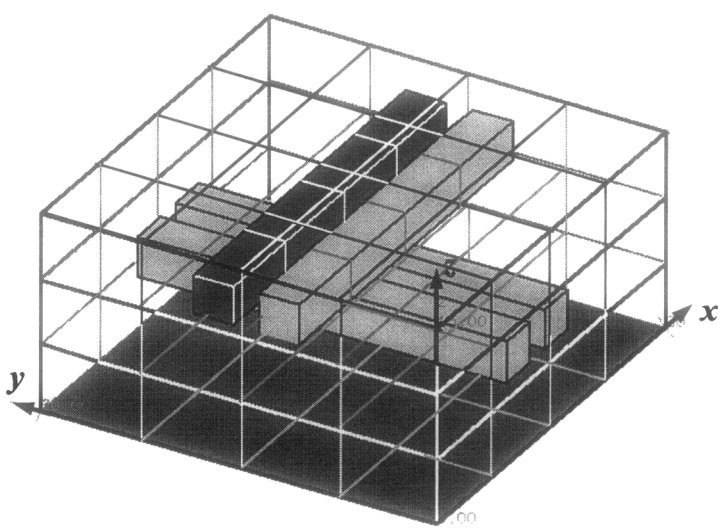

Figure 6. A 4 × 4 QMM cutting is performed on the structure of 2 × 2 crossovers.

4.2. $k \times k$ Crossovers Embedded in Three-Layered Dielectrics

The structures with $k \times k$ ($k = 2, 4, 6$) bus-crossing conductors embedded in three dielectric layers with a ground plane at the very bottom are calculated by BEM with QMM acceleration and BEM without QMM. Figure 5 shows the first structure, with 6×6 crossovers. The structure parameters are as follows. The height of each dielectric layer is 5 μm. Each metal line is a $3 \times 3 \times 28$ cube (unit in μm). The space between two adjacent metal lines on the same layer is 2 μm. The distance between the outmost metal line and the outer boundary of dielectric is 1 μm. Every metal line touches the bottom of the dielectric which surrounds it. The relative permittivities are all chosen to be 1.0 for the sake of simplicity. Removal of conductor 1, 6, 7, and 12 produces the second structure with 4×4 crossovers. And, removal of conductor 2, 5, 8, and 11 again produces the third structure with 2×2 crossovers. The capacitance between master conductor 3 and the other conductors is calculated.

Because the actual structures involve multiple dielectrics, the BEM without QMM for them uses multimedium BEM analysis in Section 2. For these cases, the analysis of optimal QMM in Section 3.3 is not applicable. A simple strategy of decomposing each dielectric layer is adopted in this experiment. Each dielectric layer is uniformly cut perpendicularly to the X-axis and Y-axis. Thus, in the top view of these structures, each layer is decomposed into an array of $m \times n$ fictitious medium blocks. Figure 6 shows the third structure is performed with 4×4 cutting. In the QMM computations of our experiment, each dielectric layer is decomposed into 6×6, 6×6, and 4×4 fictitious blocks for the three cases, respectively. The boundary element partition of these structures is using a strategy of nonuniform density partitioning to achieve high accuracy with fewer elements. So, it is hard and not necessary to describe the element partition in detail.

Table 3 shows the numbers of nonzero entries in matrix $\mathbf{A}$ and the number of iterations in the two methods. From it, we can see that BEM with QMM acceleration generates much fewer nonzero coefficients than that without QMM, so high speed-up ratio can be expected. Table 3 also shows that the number of iterations increases in the BEM with QMM acceleration.

Table 3. Comparison of the number of nonzero matrix entries and iterations for $k \times k$ crossover problem.

	BEM without QMM		BEM with QMM		Ratio of
$k \times k$	Nonzero Entry	Iteration	Nonzero Entry	Iteration	Nonzero Entry
6×6	14559975	21	1191738	27	12.2
4×4	9529903	20	993038	30	9.6
2×2	5237647	21	964454	34	5.4

Table 4 shows the capacitance, CPU time, and memory usage of both methods. For the given strategies of QMM decomposing, the BEM with QMM is about 4–10 times faster than that without QMM with the difference in the results less than 3%. And using the QMM method, the memory usage is about 2–4 times less than that not using it. The increase of iteration number shown in Table 3 should account for the difference between the actual speed-up ratio and the expected one.

Table 4. Comparison of CPU time and capacitance for $k \times k$ crossover problem.

	BEM without QMM				BEM with QMM					
$k \times k$	N-BE	Memory	Cap.	Time	N-BE	Memory	Cap.	Dis. (%)	Time	Speed-Up
6×6	5547	62	1699	161.4	6822	17	1738	2.3	16.6	9.7
4×4	4475	42	1636	104.2	5630	15	1673	2.3	14.6	7.1
2×2	3238	25	1157	56.1	3644	11	1180	2.0	13.4	4.2

5. CONCLUSIONS

Fast and accurate extraction of the parasitic interconnect capacitance from the deep submicron VLSI circuits is becoming an important and difficult task for the design of integrated circuits with high performance. A fast QMM method based on the localization of direct BEM is proposed to accelerate the BEM computation of the parasitic capacitance. The QMM method utilizes the Krylov iterative solver and takes full advantage of the localization of direct BEM. For a simplified single-medium model, an optimal Q value is analyzed, which brings the largest computational speed-up to BEM without QMM. Furthermore, the computational complexity of the QMM accelerated BEM is analyzed and concluded as an approximate linear relationship between the computational time and the number of boundary elements. The application of the QMM method

to the calculation of actual parasitic capacitance also reveals the CPU time and memory usage is greatly reduced like that for the simplified model problem.

There are some additional boundary elements partitioned on the interfaces of fictitious mediums in QMM computation, which increases the number of unknowns in the overall BEM equations. But for the problems, in which the number of unknowns on fictitious interfaces for a small percentage of the number of all unknowns, the matrix sparsity brought by the QMM method can greatly overwhelm the influence of fictitious interfaces. Otherwise, for the other problems, the QMM method may not be effective. So, the QMM method is a good choice to greatly accelerate BEM computation for the problems with most of boundary elements not related to the fictitious interfaces, like in the VLSI parasitic capacitor.

The optimal number of fictitious mediums for a single-medium problem is analyzed in this paper. The situations for some multimedium problems are much more complicated, and the optimal strategy of QMM decomposing for these problems will be discussed further in the future works.

REFERENCES

1. C.A. Brebbia, *The Boundary Element Method for Engineers*, Pentech Press, London, (1978).
2. V. Rokhlin, Rapid solution of integral equation of classical potential theory, *J. Comput. Phys.* **60**, 187–207, (1985).
3. J. Strain, Fast potential theory II: Layer potential and discrete sums, *J. Comput. Phys.* **99**, 251–270, (1992).
4. V. Rokhlin, Rapid solution of integral equations of scattering theory in two dimensions, *J. Comput. Phys.* **86**, 414–439, (1990).
5. L. Greengard and V. Rokhlin, The rapid evaluation of potential field in three dimensions, In *Vortex Methods, Lecture Notes in Mathematics 1360*, (Edited by C. Anderson and C. Greengard), Springer-Verlag, New York, (1988).
6. F.T. Korsmeyer, D.K.P. Yue, K. Nabors and J. White, Multipole-accelerated preconditioned iterative methods for three-dimensional potential problem, In *Proc. BEM'XV*, Worchester, MA, (1993).
7. J. Barnes and P. Hut, A hierarchical $O(N \log N)$ force-calculation algorithm, *Nature* **324**, 446–449, (1986).
8. A.W. Appel, An efficient program for many-body simulation, *SIAM J. Sci. Statis. Comput.* **6** (1), 85–103, (1985).
9. J. Katzenelson, Computational structure of the n-body simulation, *SIAM J. Sci. Statis. Comput.* **10** (4), 787–815, (1989).
10. W. Shi, J. Liu, N. Kakani and T. Yu, A fast hierarchical algorithm for 3-D capacitance extraction, In *Proc. 35^{th} Design Automation Conference*, pp. 212–217, (1998).
11. T. Hrycak and V. Rokhlin, An improved fast multipole algorithm for potential fields, *SIAM J. Sci. Comput.* **19** (6), 1804–1826, (1998).
12. C.L. Berman, Grid-multipole calculations, *SIAM J. Sci. Comput.* **16** (5), 1082–1091, (1995).
13. H. Chang, L. Greengard and V. Rokhlin, A fast adaptive multipole algorithm in three dimensions, *J. Comput. Phys.* **155**, 468–498, (1999).
14. A. Grama, V. Kumar and A. Semeh, Parallel hierarchical solvers and preconditioners for boundary element methods, *SIAM J. Sci. Comput.* **20** (1), 337–358, (1998).
15. Z. Wang, Y. Yuan and Q. Wu, A parallel multipole accelerated 3-D capacitance simulator based on an improved model, *IEEE Trans. Computer-Aided Design* **15** (12), 1441–1450, (1996).
16. J.H. Kane and B.L.K. Kumar, An arbitrary condensing, noncondensing solution strategy for large scale, multi-zone boundary element analysis, *Comput. Meth. Appl. Mech. Engrg.* **79**, 219–244, (1990).
17. J.B. Layton, S. Ganguly, C. Balakrishna and J.H. Kane, A symmetric Galerkin multi-zone boundary element formulation, *Int. J. Numer. Methods Engrg.* **40**, 2913–2931, (1997).
18. J.H. Kane and S. Saigal, An arbitrary multi-zone condensation technique for boundary element design sensitivity analysis, *J. AAIA* **28**, 1277–1284, (1990).
19. J.H. Kane, *Boundary Element Analysis in Engineering Continuum Mechanics*, Prentice-Hall, (1994).
20. K. Nabors and J. White, FastCap: A multipole accelerated 3-D capacitance extraction program, *IEEE Trans. Computer-Aided Design* **10** (11), 1447–1459, (1991).
21. M. Merkel, V. Bulgakov, R. Bialecki and G. Kuhn, Iterative solution of large-scale 3D-BEM industrial problems, *Engrg. Anal. Boundary Element* **22**, 183–197, (1998).
22. Y. Saad and M.H. Schultz, GMRES: A generalized minimal residual algorithm for solving nonsymmetric linear systems, *SIAM J. Sci. Statis. Comput.* **7** (3), 856–869, (1986).